Video-based assessment, predictive modelling, and SMoS for cyclist-tram track interactions

Kevin Gildea[1], Daniel Hall[1], Clara Mercadal-Baudart[1], Brian Caulfield[1], and Ciaran Simms[1]

[1]*School of Engineering, Trinity College Dublin*

Abstract

Single cyclist/bicycle collisions are common and underreported in official statistics. In urban environments, light rail tram tracks are a frequent factor, however, they have not yet been the subject of engineering analysis. The prevalence of traffic camera footage in urban environments presents an opportunity for detailed site-specific safety insights. In this study, we present a video-based frequency and risk analysis for unsuccessful crossings on tram tracks in wet road conditions at 9 locations around Dublin city centre, Ireland. We also devise a predictive model for crossing success as a function of crossing angle for use in a surrogate safety measure framework. Modelling results show that crossing angle is a strong predictor of crossing success, and that cyclist velocity is not. Findings indicate that infrastructural planners should design for cyclist crossing angles of 30°or greater. We highlight the prevalence of external factors which limit crossing angles for cyclists. In particular, kerbs are a common factor, along with passing/approaching vehicles or other cyclists. Furthermore, we introduce a new Surrogate Measure of Safety (SMoS) for cyclist interactions with tram tracks, and demonstrate its utility with an open-source application (SafeCross), which is available through the project page[1].

Keywords: single cyclist collisions, single bicycle crashes, tram tracks, video analysis, risk modelling, surrogate measures of safety

1 Introduction

The modal share of cyclist casualties among overall Road Traffic Collision (RTC) numbers has increased in recent years, reflecting an increase in popularity [Stipdonk et al., 2020]. Furthermore, underreporting of cyclist collisions to the police results in the underestimation of their societal impact [Gildea and Simms, 2021, Shinar et al., 2018, Short and Caulfield, 2014]. Single Cyclist Collisions (SCCs) or Single Bicycle Crashes (SBCs) (i.e., cases not involving an impact with another road user), are particularly underreported. The odds of police reporting for cyclist-motorised vehicle collisions (MVCs) in Ireland are estimated to be 20 times greater than SCCs [Gildea et al., 2021], similar to international estimates [Shinar et al., 2018], leading to underestimation of their importance among researchers and policymakers [Schepers et al., 2020]. For this reason, while collision/injury prevention strategies for MVCs are well-investigated, strategies for mitigating SCCs are not. A recent Irish self-reporting study has identified the most common collision configurations and factors [Gildea et al., 2021]. Findings indicate that falls involving interactions with light rail tram tracks are common in the city of Dublin , tram tracks were the most common infrastructural collision partner, and a contributing factor in 23% of single cyclist collisions (ibid.). Internationally, other self-reporting studies also highlight their importance, with 19% of cases in a study in Melbourne [Beck et al., 2019], and 13% of cases in a study in Switzerland [Hertach et al., 2018] involving tram tracks. A previous video analysis of cyclists crossing railway tracks found that the minimum safe approach angle for crossing railway tracks is 30°[Ling et al., 2017], however, this study relied on visual assessments of crossing angles (10°bins), and it is unclear whether these findings also translate to light-rail tracks where there are frequent interactions with cyclists in crowded urban

[1]https://kevgildea.github.io/SafeCross/

environments. Along with increasing popularity of cycling, many new light rail systems are being implemented across Europe as part of a broader move towards sustainable transport [UITP, 2019]. Accordingly, further investigation is required to understand potential conflicts. Due to a lack of detail in police, hospital, or insurance databases, and the prevalence of traffic cameras along tram systems, video-based approaches have obvious potential for these cases. Traffic camera footage is often used for analysis of near-collision or near-miss incidents and Surrogate Measures of Safety (SMoS) or Surrogate Safety Measures (SSM), i.e., a safety-related indicator without the need for collision footage, allowing for rapid proactive assessment of potential areas of conflict. A variety of SMoS metrics exist, e.g. Time To Collision (TTC) [Hayward, 1971], Post-Encroachment Time (PET) [Allen et al., 1978], or bicycle Deceleration Rate (DR) [Strauss et al., 2017]. Generally, these are based on vehicle trajectories (direction, velocity, acceleration), and sometimes mass (Extended Delta-V) [Laureshyn et al., 2017], which are used as proxies for collision risk. In the past, SMoS for cyclists have focused on MVCs, and similar metrics for SCCs do not exist. Validation of SMoS remains a challenge, and validation studies are rare. A common approach for validation involves comparison to historical crash data [Johnsson et al., 2021, Strauss et al., 2017]. Theoretically this may allow for prediction of expected RTC numbers, however, the problem of underreporting imposes limitations. Furthermore, the underreporting issue is of particular relevance in the context of validation for any potential SMoS metrics for SCCs. Therefore, probabilistic risk modelling with the inclusion of crash footage is the most robust approach, i.e., using an observational study design for a location/interaction of interest obtaining footage for both successful and unsuccessful cases. Therefore, in this study we aim to use traffic video to identify site-specific safety issues between cyclists and tram tracks, correlate unsuccessful crossing risk with crossing trajectories and devise a validated SMoS algorithm for future use in safety assessments.

2 Methods

2.1 Data collection

Traffic camera footage was collected in October/November 2021 following ethical approval from the School of Engineering, Trinity College Dublin. This involved manual screening, annotation and extraction of cyclist interactions with tram tracks from 9 locations (10 cameras) in Dublin city centre (Fig. 1). Locations with an established likelihood of cyclist-tram track conflicts were chosen based on findings from [Gildea et al., 2021]. We focused on weekdays, daylight conditions, and peak commuting hours [Gildea and Simms, 2021]. We initially assessed a sample that included both dry and wet conditions, but a preliminary analysis found no falls during dry conditions. Wet road conditions are a significant factor for cyclist falls on tracks [Gildea et al., 2021, Ling et al., 2017]. Therefore, we focused on periods with wet road conditions.

2.2 Track description and effective groove gap width

Various light rail track profiles exist. The popular girder grooved rail types are limited to the European standards: Ri 59N, Ri 60N, IC, Ri52N, Ri53N, NP4a, and 35G. Rail heads are similar across all types, however, the width of the groove gap differs. The Irish tram service (Luas) uses the Ri59N (Ri 59-R13) girder grooved rail in shared-space environments, i.e., most street-running sections and stops (Fig. 2). Pavement/asphalt is set around the rail to support the shared use of the road.

Larger groove gap widths present larger risks to crossing cyclists, and this is exacerbated by off-perpendicular crossing angles (<90°). This increased risk can be expressed in the form of an effective width of the groove gap (EW) when crossing at an angle (θ) [Skelton, 2016]. The relationship between θ and EW is plotted for various track types in Fig. 3, showing EW tends to infinity as angle approaches 0°. Furthermore, as crossing angle reduces the differences between effective widths of the track types widens.

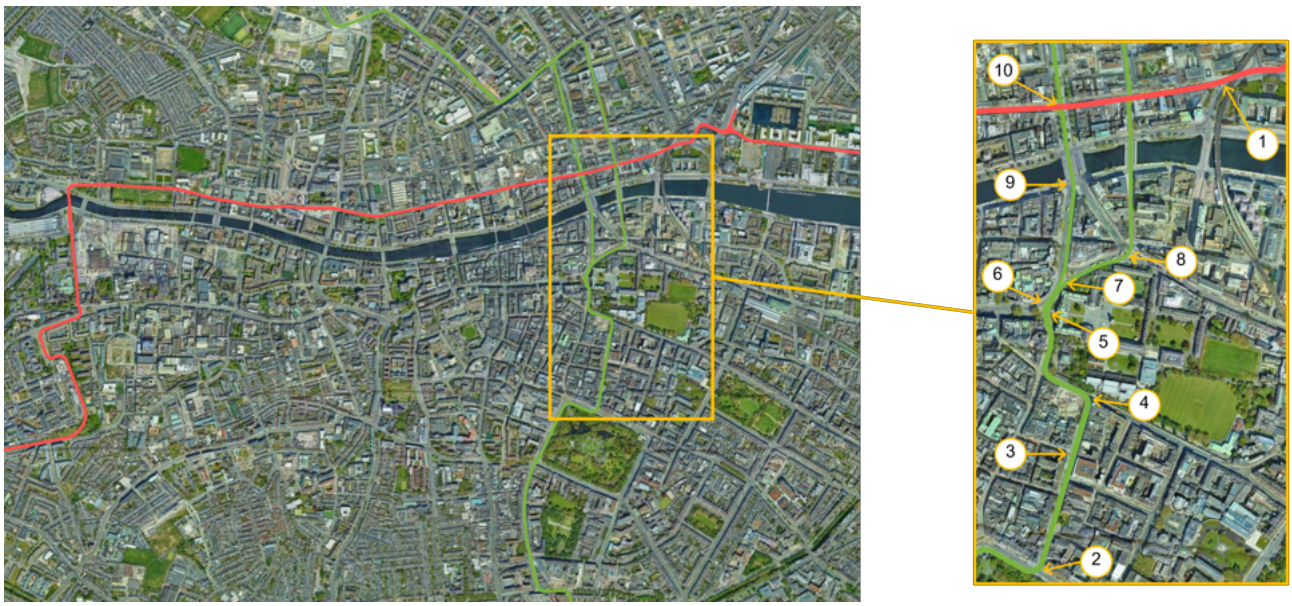

Figure 1: Study locations in Dublin city centre.

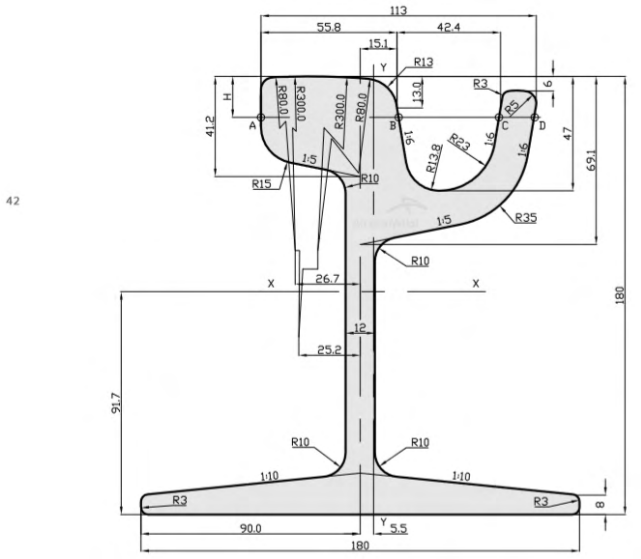

Figure 2: Profile of the 59R2 (Ri59N) grooved rail.

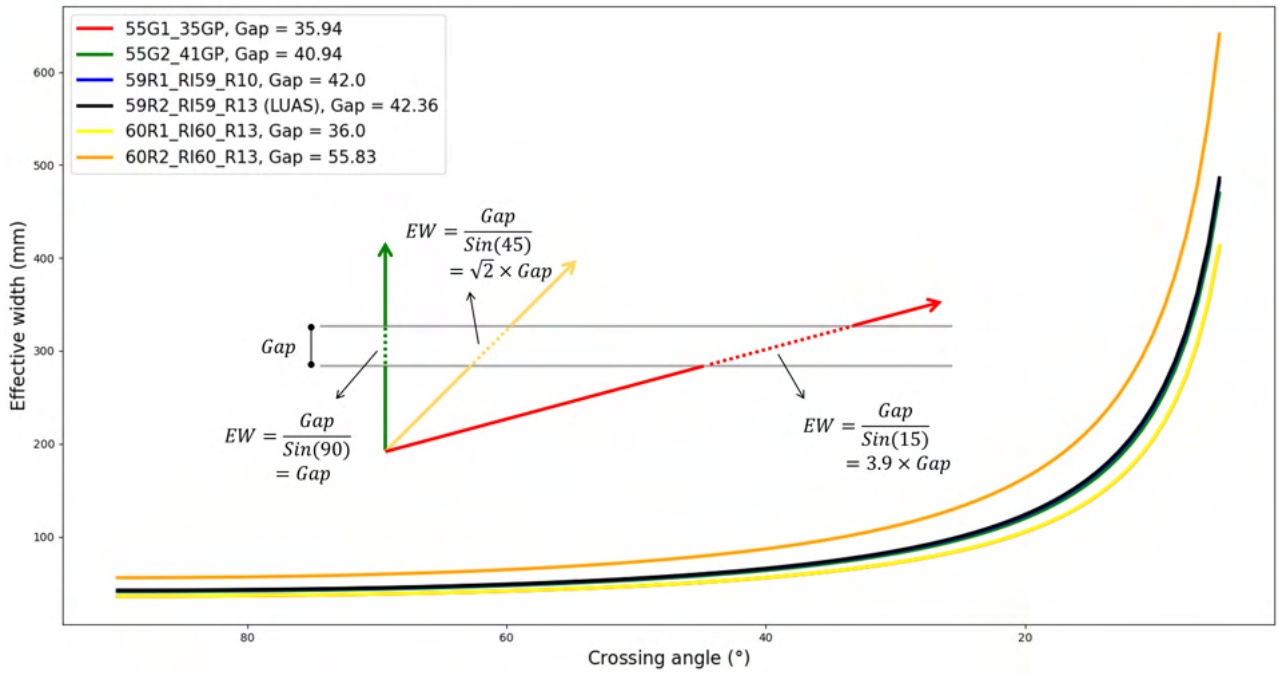

Figure 3: Effective track groove gap width (EW) by crossing angle (θ) for various track types. Some of the curves overlap.

2.3 Frequency and risk analysis

Using the collected footage, exposure and time-based risk analyses were performed to assess the rate of Unsuccessful Crossings (UCs) compared to Successful Crossings (SC) at each recording site. UCs are here defined as falls and near-falls involving evidence of loss of control.

2.4 Fall type taxonomy

We define three broad categories for UCs (Fig. 4).

2.5 Crossing angles and trajectories

Footage of UCs, and a random sample of SCs were extracted for analysis. T-Analyst software (developed in the European InDev project[2]) was used to calculate cyclist velocities and trajectories [Johnsson et al., 2018]. In this framework, T-calibration allows for ground-plane calibration of monocular traffic camera footage from manually annotated scene points in both the traffic camera footage and a satellite image (with scale) of the recording location (e.g. Google Earth) [Tsai, 1987] (see Fig. 5). Once calibrated, 3D bounding boxes were annotated for each frame, corresponding to discrete cyclist positions over time on the X-Y plane (ground). Tracks were annotated in a similar way, using points on the ground plane. For cases involving straight tracks a cardinal axis along the track was defined during calibration, and for curved tracks pixel coordinates were annotated along the track and a 2nd order polynomial was fitted in post-processing. For calculation of crossing angles (0-90°) and velocities (m/s), a time window was defined based on visual inspection using frames before and after crossing for SCs and only frames before crossing for UCs. Crossing angles were calculated as angles between line segments representing the track and the cyclist trajectory at that location. Frame-based velocity estimates were calculated from trajectories using the central difference method and the camera framerate, and

[2]https://cordis.europa.eu/project/id/635895/

Figure 4: The three defined categories for unsuccessful crossings (UCs).

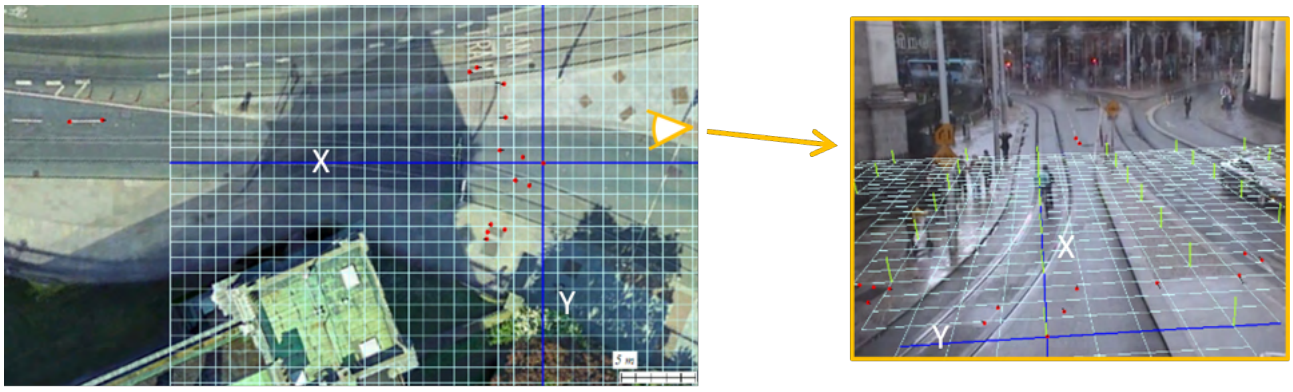

Figure 5: Ground plane calibration for Westmoreland St./College St. (Camera 7).

averaged across the window. Cases were excluded if the view of the cyclist was obstructed, the initial track interaction occurred out of frame, or if tracking confidence was affected by distance from the camera (image or calibration quality).

2.6 Statistical analysis and predictive modelling

Binary logistic regression modelling was used to establish the combined effects of crossing angle and velocity on crossing success (Eqn. 1).

$$p = P(Y = 1|X = x_1, \ldots, X_i = x_i) = \frac{e^{\alpha+\beta_1 x_1 \cdots+\beta_i x_i}}{1+e^{\alpha+\beta_1 x_1 \cdots+\beta_i x_i}} \quad (1)$$

where the dependent variable Y takes two values (1, 0), β_i are the coefficients estimated using the method of maximum likelihood and x_i are the predictor variables. In modelling, we used a random sample of SCs across the study locations. To satisfy the assumption of 'independence of observations', only one crossing of one track is included for each cyclist. We considered both effect estimation and predictive modelling, and created

Camera	No. cyclists	Hours	UC	UC/No. cyclists	UC/Hour
1	198	7	1	0.005	0.143
2	145	7	0	0	0
3	181	7	1	0.005	0.143
4	116	7	0	0	0
5&6	410	7	1	0.002	0.143
7	377	12	8	0.021	0.667
8	324	7	1	0.003	0.143
9	551	7	1	0.002	0.143
10	603	7	0	0	0
Total	2,905	68	13	0.004	0.191

Table 1: Summary description of the study data, and UC risk estimates.

three models, one for effect estimation (a) and two for predictive modelling (b c). Model (b) was derived using crossing angle (θ) as the independent variable (IV), whereas for model (c) θ was transformed into EW (Fig. 3). For effect estimation (model (a)), we included all variables, while for predictive modelling we included only significant variables [Harrell, 2015]. A Pearson correlation coefficient was computed to determine the relationship between IVs, indicating non-significant relationships between velocity and (1) (r(108) = -0.046, p=0.64), and (2) EW (r(108) = -0.008, p=0.936). The IVs were found to be linearly related to the logit of the dependent variable (crossing success) via the Box-Tidwell procedure, with $p > 0.05$. No outliers were found (absolute value of standardised residual greater than 2.5). Predictive models are used in the definition of a SMoS for cyclist-tram track interactions. For this purpose, we define Eqn. 2 for predicting the number of UCs (N_{UC}) at a site over a period of time using a representative random sample of estimated crossing angles ($\theta = [\theta_1, \ldots, \theta_M]$), and a count of cyclist numbers (N_C).

$$N_{UC} = N_C \times \frac{1 - \frac{e^{\alpha+\beta x}}{1+e^{\alpha+\beta x}}}{M} \tag{2}$$

where α, β are taken from the modelling, and $\underline{x} = \underline{\theta}$ for model (b), or $\left[\frac{Gap}{sin(\theta_1))}, \ldots, \frac{Gap}{sin(\theta_M))}\right]$ for model (c).

3 Results

3.1 Data summary

Table 1 shows a summary of the collected data. A total of 2,905 cyclist interactions with tram tracks were surveyed over two periods with wet road conditions. Extracted footage includes 13 UCs (4 Cat. 1, 5 Cat. 2, and 4 Cat. 3 – see Table 3), and a random sample of the total (2,891) SCs. A total of 9 UCs were identified over Period 1 (7 hours) out of 2,741 cyclists, corresponding to an UC rate of $3.3\text{x}10^{-3}$ (approx. 3 in a 1000). A higher rate was observed in Camera 7 (Westmoreland St./College St.) (4 UCs for 213 cyclists), and a further 5 hours of footage was examined in this location (Period 2), during which a further 4 UCs were noted. Overall, this location has a UC rate of $2.1\text{x}10^{-2}$, or 21 in 1,000.

3.2 Site study: Camera 1

The majority of crossings at this location (Abbey St./Beresford St.) were at the nearside of the road at a safe crossing angle ($\overline{\theta} = 38°$) (Fig. 6). The single fall at this location occurred further down the tracks where the cyclist travelled more parallel to the tracks, and was passed by a motorised vehicle while crossing ($\theta = 14°$) (Fig. 7).

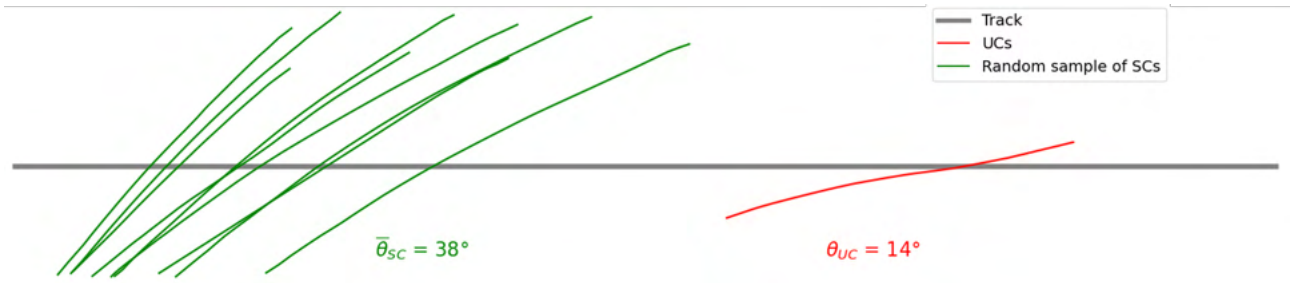

Figure 6: Trajectory analysis of cyclist interactions with a track at Abbey St./Beresford St. (Camera 1).

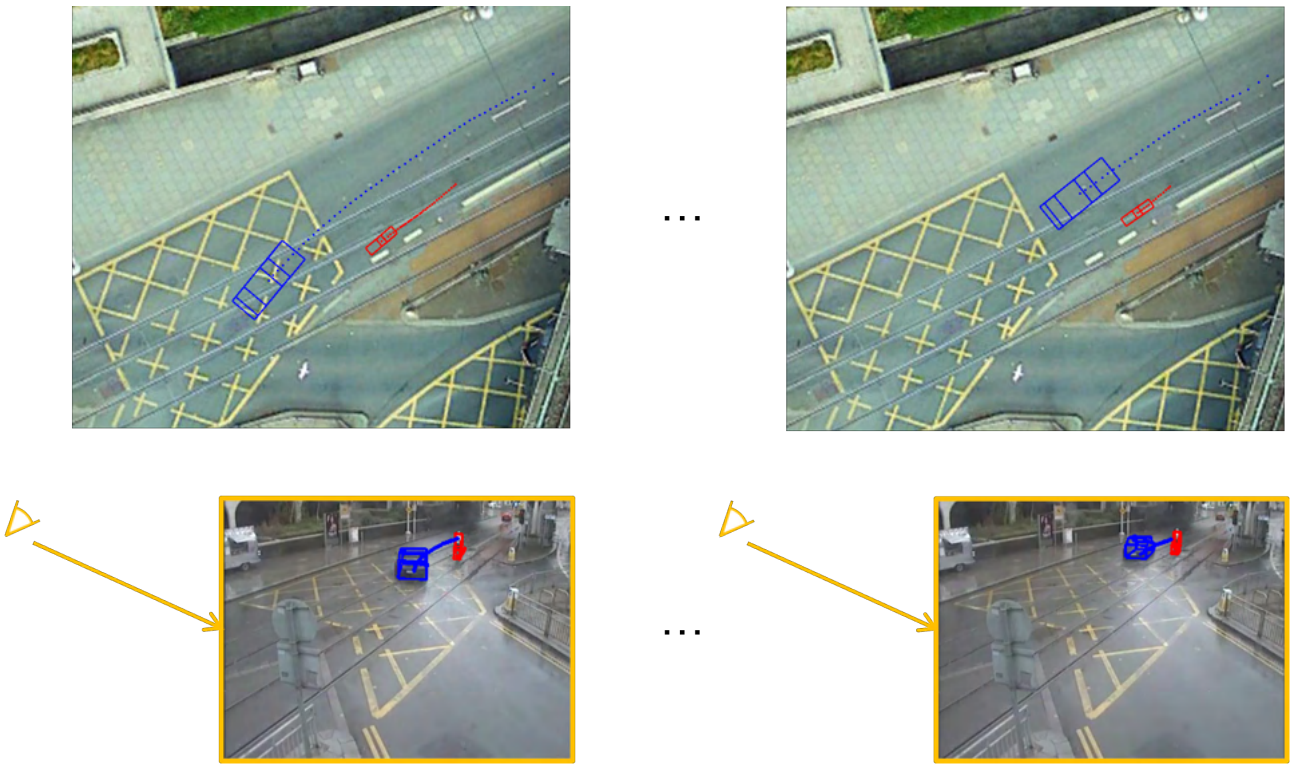

Figure 7: Cat. 3 fall at Abbey St./Beresford St. (Camera 1).

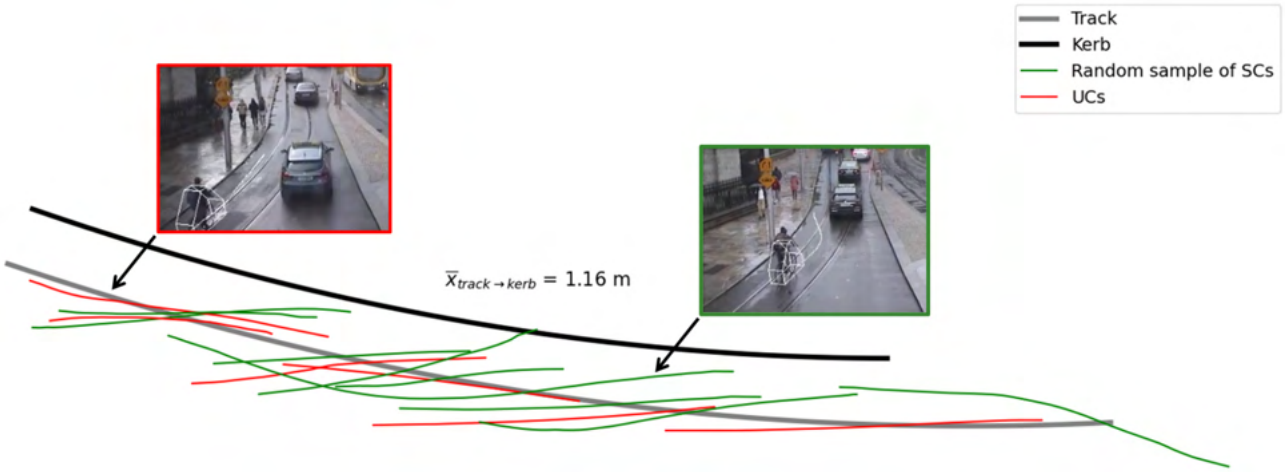

Figure 8: Trajectory analysis of cyclist interactions with the inside track at Westmoreland St./College St. (Camera 7).

3.3 Site study: Camera 7

Most UCs at this location occurred on the inside track (N=7, 87%), and the analysis focused on these cases. Trajectories of 6 UCs and a random sample of 7 SCs over the inside track were annotated for Camera 7 (Fig. 8). Mean crossing angles were higher for SCs ($\overline{\theta}$ = 17°, SD = 3.5), compared to UCs ($\overline{\theta}$ = 10°, SD = 5.9). The results of a Mann-Whitney U test indicate significant difference between groups (U = 8, p = 0.03). Average velocities were similar: 4.2m/s for SCs vs. 4.0m/s for UCs. Falls on the inside kerb were common, and crossing angles were low for both SCs and UCs (≤ 20°- excluding one case with intentional mounting of the kerb). This is likely due to the proximity of the nearside kerb (1.16m from the track on average), which limits crossing angle.

3.4 Multivariable testing and predictive modelling for crossing success

Vectors representing the trajectories for UCs and SCs included in the modelling analysis are shown in Fig. 9. Mean crossing angles and velocities (and their standard deviations) are also included. Mean crossing angles are notably shallower for UCs (10°vs. 43°), while mean velocities are very similar (4.7m/s vs. 4.8m/s).

3.4.1 Model (a) Effect Estimation

Binary logistic regression modelling was used to assess the combined effect of crossing angle and velocity, and to define a predictive model for crossing success. Only crossing angle was significant, see Table 4. The model was statistically significant $\chi^2(2) = 39.017$, $p < 1x10^{-8}$, Nagelkerke R^2: 74%.

3.4.2 Model (b) Predictive Modelling Using crossing angle as IV

Model (b) was also statistically significant, $\chi^2(1) = 37.980$, $p < 1x10^{-9}$, Nagelkerke R^2: 72% (Fig. 10). It correctly classified 96% of cases, and the area under the Receiver Operating Characteristic (ROC) curve was 0.98 (95% CI: 0.956-1.000) (Fig. 14), considered an outstanding level of discrimination [Hosmer et al., 2013].

SC probabilities for various crossing angles based on model (b) are shown in Fig. 11. Results place the boundary for the definition of a minimum 'safe' crossing angle in the region of 25-30°. Below this, the probability of a SC decreases dramatically. Most notably, between 17.5°and 10°the probability of a SC drops from 0.85 to 0.22.

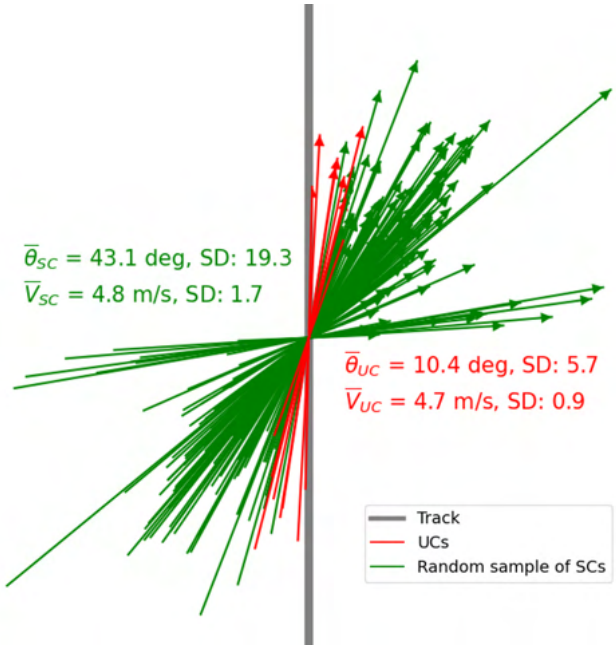

Figure 9: Crossing angles and velocities (vector magnitudes).

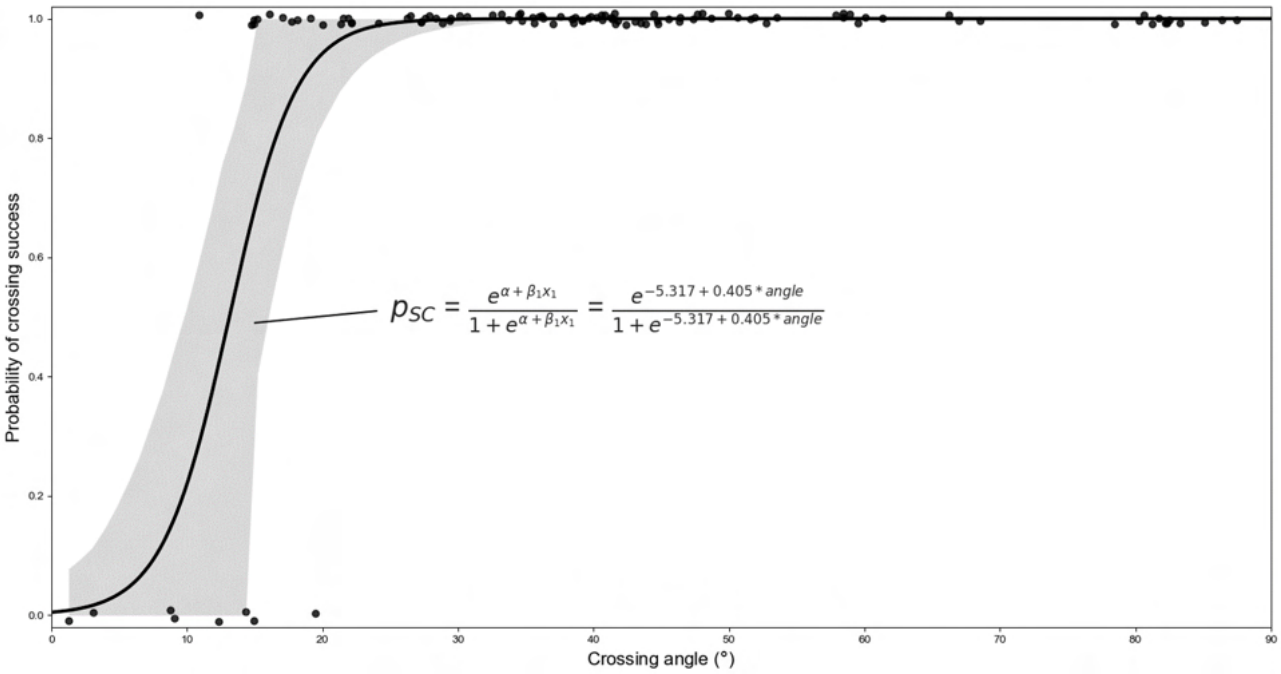

Figure 10: SC probability risk curve by crossing angle with 95% confidence levels for model (b).

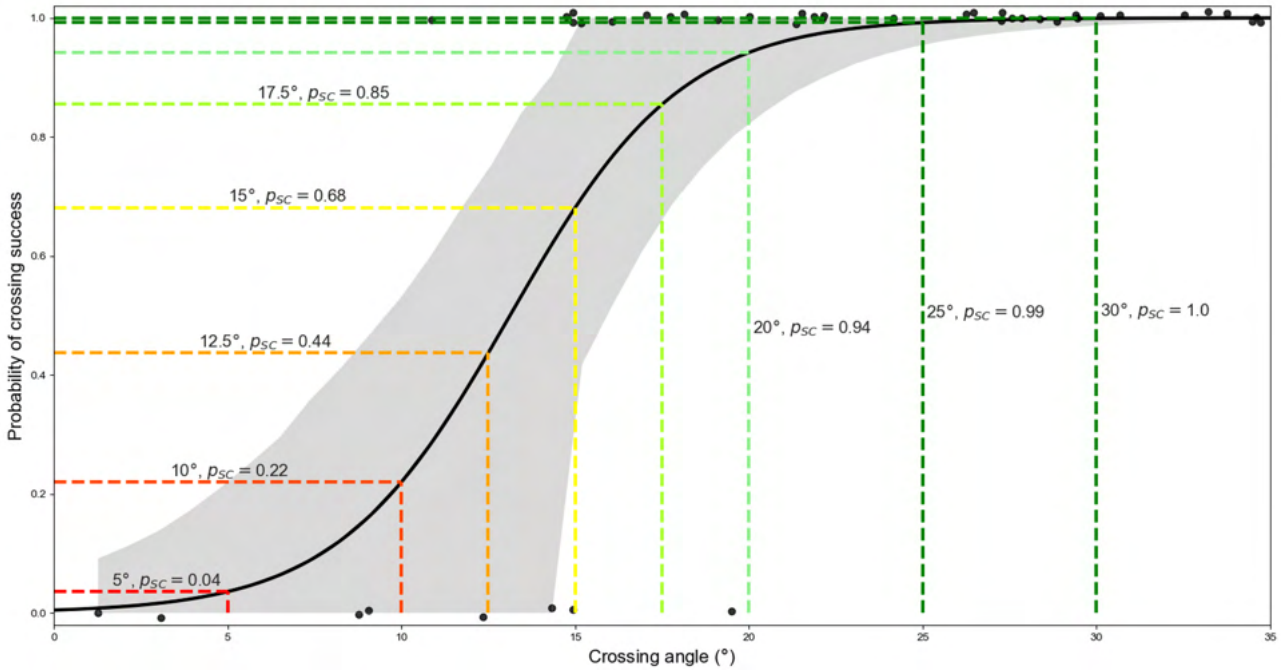

Figure 11: SC probabilities for various crossing angles from model (b).

3.4.3 Model (c) Predictive Modelling Using EW as IV

Model (c) was also statistically significant, $\chi^2(1) = 33.987$, $p < 1x10^{-8}$, Nagelkerke R^2: 70%, and the area under the Receiver Operating Characteristic (ROC) curve was the same as model (b) 0.98 (95% CI: 0.956-1.000). Using this, we can define approximate risk curves for a variety of track types (Fig 12).

SC probabilities for various crossing angles based on model (c) are shown in Fig. 13, showing slightly different results to model (b) (Fig. 11). Although these findings also place the boundary for minimum 'safe' crossing angles in the region of 25-30°, for lower crossing angles the associated SC probabilities drop more rapidly. For example, between 17.5°and 10°the probability of a SC drops from 0.9 to 0.1.

3.5 Application of predictive models for SMoS

Section 3.4 showed there are some differences in risk curves between predictive models (b) and (c). Table 2 shows the effect of the chosen model on the prediction of UC numbers, i.e. in the application of Eqn. 2. Although the models deviate somewhat for shallower crossing angles (<25°), in application they predict very similar N_{UC} levels.

4 Discussion

We observed a high overall incidence numbers for UCs over this short study period with limited coverage of the track network, highlighting the significance of the safety issue. These findings support results from a self-reporting collision survey [Gildea et al., 2021]. One location had a particularly high risk (Camera 7: Westmoreland St./College St), and an additional UC was noted for an adjacent study location (Cameras 5&6: College Green). Overall UC rates were approx. 21/1000 cyclists at Camera 7, vs. approx. 3/1000 overall. These findings are similar to a study in the US for railway tracks, which found fall rates of 2/1000 at one location, and 15/1000 at another [Ling et al., 2017], from a sample including over 13,000 cyclist traversings over a 2 month period. By comparison, the sample in this study was over only 7 hours over 8 locations around

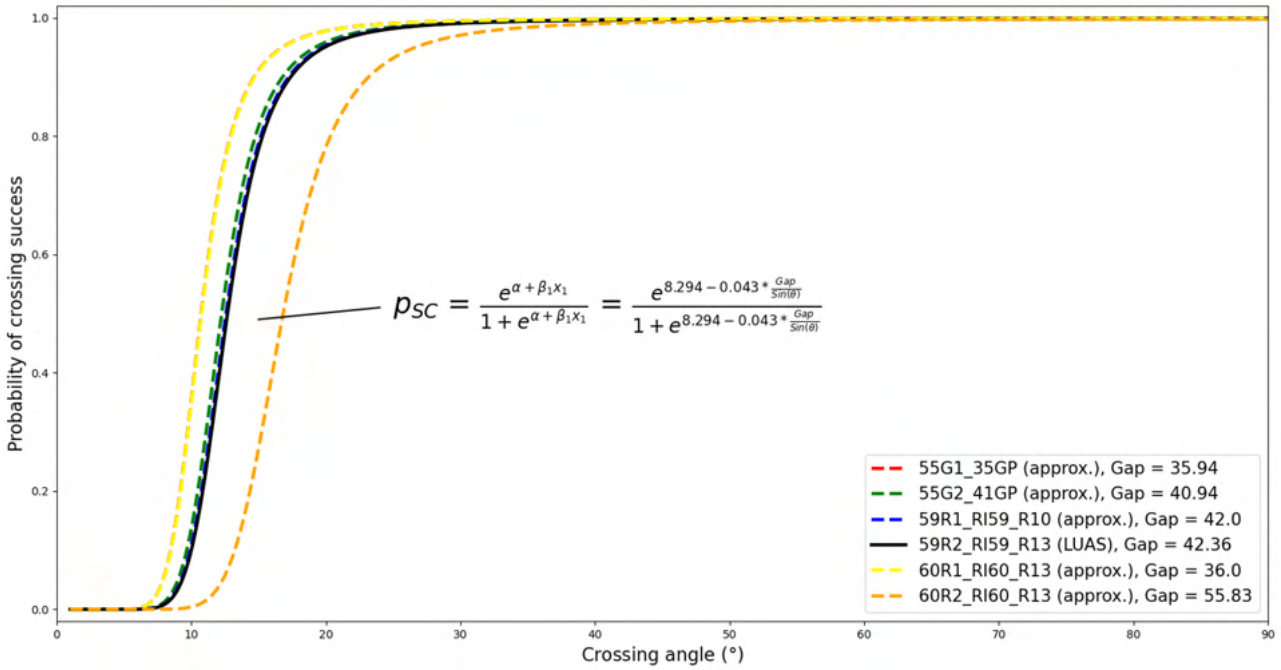

Figure 12: Approximate SC probability risk curves for various track types, vs. crossing angle, calculated as a function of effective track width from model (c).

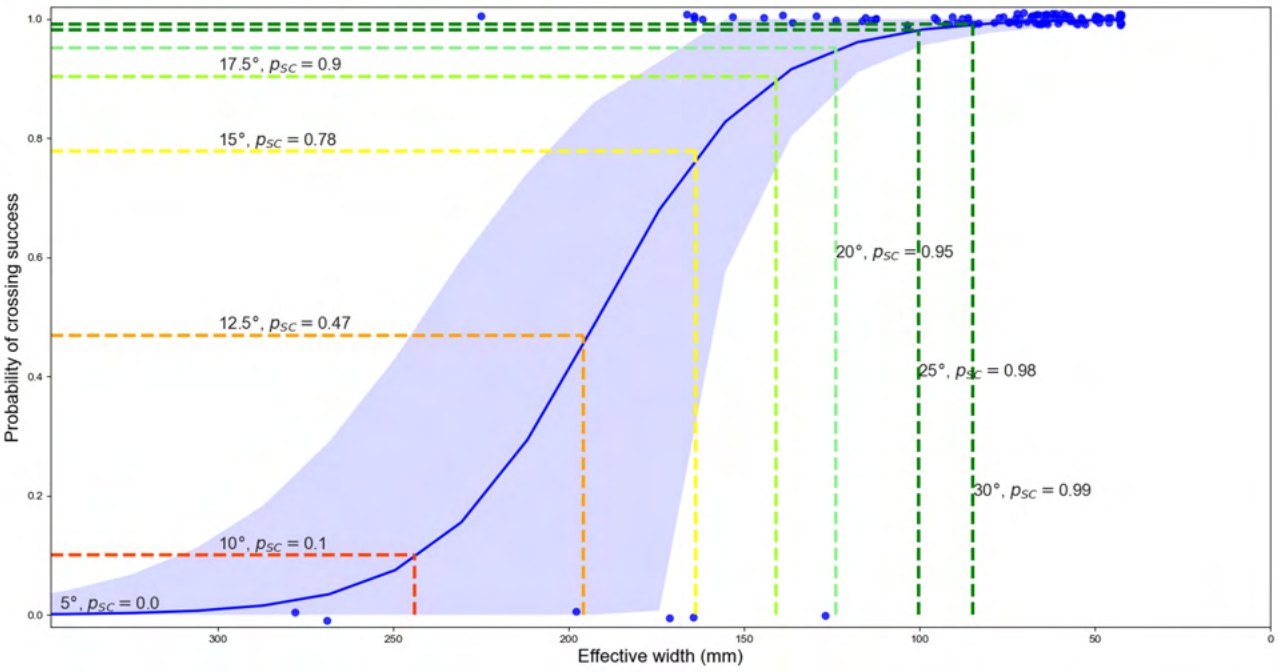

Figure 13: SC probabilities for various crossing angles from model (c) (Groove gap = 42.36mm).

θ range	Model (b)	Model (c)	% diff
0-10°	946	993	2%
0-20°	614	617	0%
0-30°	527	537	1%
0-40°	327	336	1%
0-50°	309	322	2%
0-60°	268	269	0%
0-70°	145	149	1%
0-80°	142	149	2%
0-90°	191	194	1%

Table 2: Predicted numbers of UCs for models (b) and (c), where N_C=1,000, and M=100, with randomly generated angles ($\underline{\theta}$) within a stated range.

the city (plus an added 5 hours for camera 7). At Camera 7: Westmoreland St./College St, the majority of UCs (N=7, 87%) occurred on the inside/nearside track where a kerb runs alongside in close proximity (see section 3.3). UCs at this location are likely due to the proximity of this kerb. All crossings in this location (including both UCs and SCs) are far below the mean crossing angle seen across other locations. For SCs, crossing angles at this location were an average of 17°vs. 43°overall. Extending the roadway at this location to allow for safe crossing angles would likely have a significant impact on the fall rates. The authors recommend physical separation of cyclists from tram tracks, and at locations where cyclists are expected to cross tracks, sufficient space should be available for a safe approach angle. Furthermore, since by visual inspection, most (N=12, 92%) UCs at other locations involve obstacles that limit crossing angle, i.e. kerbs or nearby/passing vehicles/other cyclists (Table 3). Furthermore many cases involve a passing/nearby motorised vehicles (N=4, 31%). Therefore, the authors recommend efforts to increase priority for cyclists at crossings, and provision of segregated lanes where possible. Descriptive statistics (Fig. 9) show that while mean crossing velocities are similar across SCs and UCs (4.8m/s vs. 4.7m/s), mean crossing angles were not (43°vs. 10°). Therefore, as expected, from multivariable modelling, crossing angle was found to be a strong predictor of crossing success. Though crossing velocity was not a significant predictor (Table 4), similar to [Ling et al., 2017], it is possible that velocity could factor into a multiclass predictive model. With this in mind, a multinomial regression was performed with crossing categories, i.e., a dependent variable with 4 levels (SC, UC-Cat. 1, UC-Cat. 2, UC-Cat. 3), however, the model was not statistically significant and had low discrimination. With a greater sample size, such a model may reveal predictive effects. As described in section 3.4, of the two predictive models (b & c), there are slight differences in risk curves. Specifically, while both models indicate that the boundary for the definition of a minimum 'safe' crossing angle in the region of 30°, SC probabilities vary below this. These differences are tested in the context of a potential SMoS for prediction of UC numbers (NUC) in section 3.5, showing that both models predict similar numbers in application. Model (c) generally predicts a slightly higher number. Furthermore, model (c) allows for approximate risk estimates for crossings on tracks with different groove gap widths. Infrastructural planners should plan for road designs that allow for and encourage crossing angles of 30°or more. However, for site-specific infrastructural planning it may be difficult to account for all common cyclist trajectories. Our findings indicate that predictive modelling of UCs on tram tracks could be used in a framework for SMoS.

5 Conclusions

We present the first video-based trajectory and fall analysis for cyclist interactions with light rail tram-tracks. Our analysis focuses on wet road conditions as a common and safety-critical edge case. We highlight actionable site-specific safety issues at location in Dublin city centre, and model the risk of UC occurrence by crossing angle. As evident by the prevalence of external factors limiting crossing angle (e.g. kerbs, other road users), personal responsibility/educational campaigns targeted towards cyclists are unlikely to address the majority of

falls on tracks. In the context of the Safe System approach, these findings imply the need for bolstered data collection regimes in urban environments, and engineering interventions to facilitate safe crossing angles. The use of the validated SMoS algorithm developed in this study can help achieve these goals, and we provide an open-source application for this purpose (SafeCross[3]).

Acknowledgements

This research was funded under the RSA-Helena Winters Scholarship for Studies in Road Safety.

[3] https://kevgildea.github.io/SafeCross/

References

[Allen et al., 1978] Allen, B., Shin, T., and Cooper, P. (1978). Analysis of traffic conflicts and collisions. *Transportation Research Record*, 667:67–74.

[Beck et al., 2019] Beck, B., Stevenson, M. R., Cameron, P., Oxley, J., Newstead, S., Olivier, J., Boufous, S., and Gabbe, B. J. (2019). Crash characteristics of on-road single-bicycle crashes: An under-recognised problem. *Injury Prevention*.

[Gildea et al., 2021] Gildea, K., Hall, D., and Simms, C. (2021). Configurations of underreported cyclist-motorised vehicle and single cyclist collisions: Analysis of a self-reported survey. *Accident Analysis Prevention*, 159:106264.

[Gildea and Simms, 2021] Gildea, K. and Simms, C. (2021). Characteristics of cyclist collisions in Ireland: Analysis of a self-reported survey. *Accident Analysis Prevention*, 151:105948.

[Harrell, 2015] Harrell, F. E. (2015). *Regression Modeling Strategies*. Springer Series in Statistics. Springer International Publishing.

[Hayward, 1971] Hayward, J. (1971). *Near Misses as a Measure of Safety at Urban Intersections - John Charles Hayward*. PhD thesis, Pennsylvania State, USA.

[Hertach et al., 2018] Hertach, P., Uhr, A., Niemann, S., and Cavegn, M. (2018). Characteristics of single-vehicle crashes with e-bikes in Switzerland. *Accident Analysis Prevention*, 117:232–238.

[Hosmer et al., 2013] Hosmer, D. W., Lemeshow, S., and Sturdivant, R. X. (2013). *Applied logistic regression.*

[Johnsson et al., 2021] Johnsson, C., Laureshyn, A., and Dágostino, C. (2021). Validation of surrogate measures of safety with a focus on bicyclist–motor vehicle interactions. *Accident Analysis Prevention*, 153:106037.

[Johnsson et al., 2018] Johnsson, C., Norén, H., Laureshyn, A., and Ivina, D. (2018). InDev Deliverable 6.1: T-Analyst - semi-automated tool for traffic conflict analysis. Technical report.

[Laureshyn et al., 2017] Laureshyn, A., de Goede, M., Saunier, N., and Fyhri, A. (2017). Cross-comparison of three surrogate safety methods to diagnose cyclist safety problems at intersections in Norway. *Accident Analysis and Prevention*, 105:11–20.

[Ling et al., 2017] Ling, Z., Cherry, C. R., and Dhakal, N. (2017). Factors influencing single-bicycle crashes at skewed railroad grade crossings. *Journal of Transport Health*, 7:54–63.

[Schepers et al., 2020] Schepers, P., de Geus, B., van Cauwenberg, J., Ampe, T., and Engbers, C. (2020). The perception of bicycle crashes with and without motor vehicles: Which crash types do older and middle-aged cyclists fear most? *Transportation Research Part F: Traffic Psychology and Behaviour*, 71:157–167.

[Shinar et al., 2018] Shinar, D., Valero-Mora, P., van Strijp-Houtenbos, M., Haworth, N., Schramm, A., De Bruyne, G., Cavallo, V., Chliaoutakis, J., Dias, J., Ferraro, O., Fyhri, A., Sajatovic, A. H., Kuklane, K., Ledesma, R., Mascarell, O., Morandi, A., Muser, M., Otte, D., Papadakaki, M., Sanmartín, J., Dulf, D., Saplioglu, M., and Tzamalouka, G. (2018). Under-reporting bicycle accidents to police in the COST TU1101 international survey: Cross-country comparisons and associated factors. *Accident Analysis Prevention*, 110:177–186.

[Short and Caulfield, 2014] Short, J. and Caulfield, B. (2014). The safety challenge of increased cycling. *Transport Policy*, 33:154–165.

[Skelton, 2016] Skelton, D. (2016). Tram/Cycle infrastructure Review Study. Technical report, Sheffield City Council.

[Stipdonk et al., 2020] Stipdonk, H., Sanz-Villegas, M. T., Thomas, P., Velten, B., Foundation, D., Yannis, G., Avenoso, A., and Jost, G. (2020). How safe is walking and cycling in Europe? Technical report, European Transport Safety Council.

[Strauss et al., 2017] Strauss, J., Zangenehpour, S., Miranda-Moreno, L. F., and Saunier, N. (2017). Cyclist deceleration rate as surrogate safety measure in Montreal using smartphone GPS data. *Accident Analysis Prevention*, 99:287–296.

[Tsai, 1987] Tsai, R. Y. (1987). A Versatile Camera Calibration Technique for High-Accuracy 3D Machine Vision Metrology Using Off-the-Shelf TV Cameras and Lenses. *IEEE Journal on Robotics and Automation*, 3(4):323–344.

[UITP, 2019] UITP (2019). Light rail and tram: The European outlook. Technical report.

Appendices

Case 1

- Camera 1
- Cat 3.

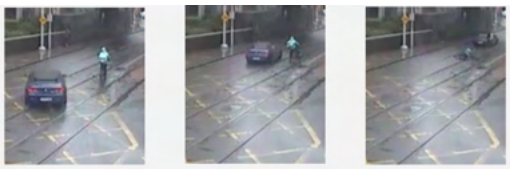

Case 2

- Camera 3
- Cat 2.

Case 3

- Camera 5
- Cat 2.

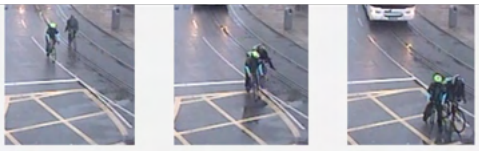

Case 4

- Camera 7
- Cat 2.

Case 5

- Camera 7
- Cat 2.

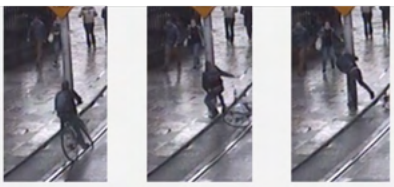

Case 6

- Camera 7
- Cat 3.

Case 7

- Camera 7
- Cat 1.

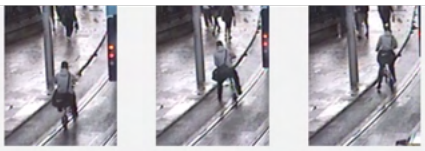

Case 8

- Camera 7
- Cat 1.

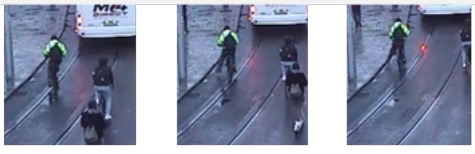

Case 9 • Camera 7 • Cat 3.		
Case 10 • Camera 7 • Cat 1.		
Case 11 • Camera 7 • Cat 2.		
Case 12 • Camera 8 • Cat 3.	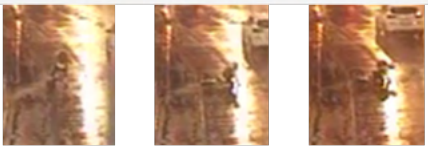	
Case 13 • Camera 9 • Cat 1.		

Table 3: All UCs noted in this study.

							95% C.I.for Exp()	
		S.E	Wald	df	Sig.	Exp()	Lower	Upper
Crossing angle	.489	.215	5.152	1	.023	1.630	1.069	2.486
Velocity	.671	.745	.812	1	.368	1.957	.454	8.431
Constant	-9.621	5.804	2.748	1	.097	.000		

Table 4: Results for regression model (a).

							95% C.I.for Exp()	
		S.E	Wald	df	Sig.	Exp()	Lower	Upper
Crossing angle	.405	.161	6.328	1	.012	1.500	1.094	2.057
Constant	-5.317	2.478	4.605	1	.032	.005		

Table 5: Results for regression model (b).

							95% C.I.for Exp()	
		S.E	Wald	df	Sig.	Exp()	Lower	Upper
EW	-.043	.014	9.949	1	.002	.958	.932	.984
Constant	8.294	2.170	14.608	1	.000132	4000.460198		

Table 6: Results for regression model (c).

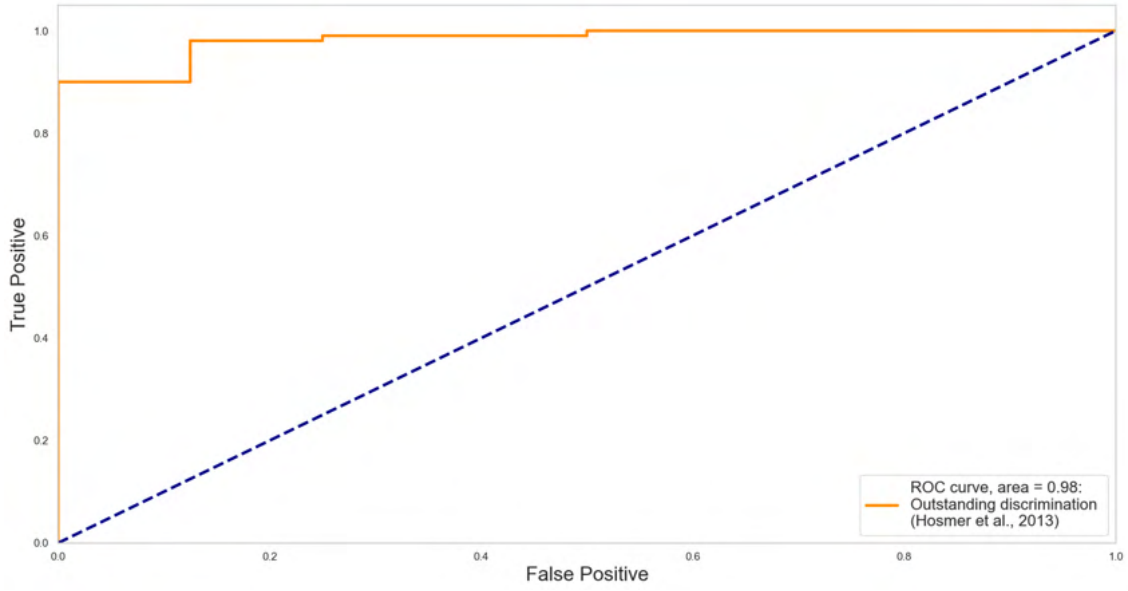

Figure 14: Receiver Operating Characteristic (ROC) curve for model (b).